Investigation of the Adsorption of L-Cysteine on a Polycrystalline Silver Electrode by Surface-Enhanced Raman Scattering (SERS) and Surface-Enhanced Second Harmonic Generation (SESHG)

Alexandre G. Brolo,* Patrick Germain, and Gabriele Hager

Department of Chemistry, University of Victoria, P.O Box 3065, Victoria, British Columbia V8W 3V6, Canada

Received: February 16, 2002; In Final Form: April 15, 2002

The adsorption of L-cysteine (L-Cys) onto a polycrystalline silver electrode surface was investigated by in situ spectroelectrochemical methods. Surface-enhanced Raman spectroscopy (SERS) and surface-enhanced second-harmonic generation (SESHG) measurements were performed in a 0.2 M KCl solution in the presence and absence of L-Cys. The experimental results indicated that L-Cys strongly adsorbs onto silver and remains on the surface at potentials as negative as −900 mV (vs Ag/AgCl). A peak around −650 mV was observed in the SESHG intensity versus applied potential plots obtained in the presence of L-Cys. The peak was indicative of an abrupt change in the electronic properties of the interface at that potential. The SERS spectra at potentials more negative than ca. −650 mV showed an increase in the intensity of vibrational modes assigned to the carboxylate group of L-Cys. The combination of the SERS and the SESHG results suggests a potential-induced reorientation of the adsorbed L-Cys molecules for potentials more negative than −650 mV. The data interpretation considered the different possible conformational forms of L-Cys adsorbed on the Ag surface. At potentials more positive than ca. −650 mV, L-Cys molecules adsorb with the protonated amino group pointing toward the surface. In this case, the positively charged amino group is stabilized by the coadsorbed chloride anions. The molecule changes its conformation at potentials more negative than −650 mV as the chloride ions leave the surface. The $C_\alpha-C_\beta$ bond rotation brings the carboxylate group closer to the surface at these potentials.

1. Introduction

Organosulfur compounds (including those with sulfhydril and disulfide moieties) are able to attach strongly to certain metallic surfaces, creating modified interfaces with unique properties. L-cysteine (L-Cys) is an amino acid with a thiol side chain ($HSCH_2CHNH_2COOH$) that spontaneously self-assembles on gold and silver electrodes.[1] These modified metallic surfaces may find significant technological applications in several areas such as chemical-specific sensing and catalysis. For instance, proteins can be readily immobilized on L-Cys-coated surfaces, yielding very convenient substrates for nanofabrication and patterning involving biological materials.[2] A better understanding of the molecular properties of L-Cys monolayers would certainly help in recognizing the parameters that govern the protein adhesion. The characterization of the monolayer in an electrochemical environment would also be advantageous because proper control over the electrical potential of the interface should allow better regulation of the protein adsorption.

The electrochemistry of L-Cys on several types of electrode materials has been widely investigated.[3,4] For instance, mechanisms for the electro-oxidation of cysteine on polycrystalline and low index single-crystalline gold electrodes have been suggested.[4] A comprehensive review of the early literature has also been published.[1]

In situ (in an electrochemical environment) scanning tunneling microscopy (STM) characterizations of L-Cys adlayers on Au(111) have been performed.[5−7] The microscopic structure revealed in these works showed that L-cysteine molecules form highly ordered monolayers. The papers, however, do not agree on an adlayer structure.

The structural arrangement of adsorbed L-Cys on both copper and gold electrodes has also been investigated using ex situ (not in an electrochemical environment) surface spectroscopic methods.[8,9] X-ray photoelectron spectroscopy (XPS) has confirmed strong dissociative chemisorption involving the thiol group.[9] Infrared reflection absorption spectroscopy (IRAS) data has suggested that $-SCH_2CHNH_3^+COOH$ should be the predominant form adsorbed at lower pH values (pH = 1.5 and 5.7). The $-SCH_2CHNH_2COO^-$ form should be at the surface at pH 11.7.[8] The adsorption of the zwitterionic form ($-SCH_2CHNH_3^+COO^-$) has been clearly demonstrated by the SERS of L-Cys adsorbed on silver colloids.[1] SERS studies of L-Cys adsorbed on silver electrodes are the only reports on the in situ spectroelectrochemical characterization of the adsorption of this amino acid.[1,12] Watanabe and Maeda confirmed a very strong adsorption on silver through the sulfur group.[11] Stewart and Fredericks concluded that the ionized carboxylate group and the protonated amino group were also in close contact with the surface.[12] Neither of these previous electrochemical SERS studies focused on the dependence of the molecular orientation with respect to the applied potential.

A combination of electrochemistry and in situ spectroelectrochemical methods (SERS and SESHG) was used in this study to investigate the potential-dependent adsorption of L-Cys on a silver electrode. The vibrational characteristics of the adsorbed molecule are readily obtained by SERS. SESHG is very sensitive to changes in the electronic structure of the interface. Therefore, the essentially complementary information provided by both

* Corresponding author. E-mail: agbrolo@uvic.ca.

10.1021/jp025650z CCC: $22.00
Published on Web 05/18/2002

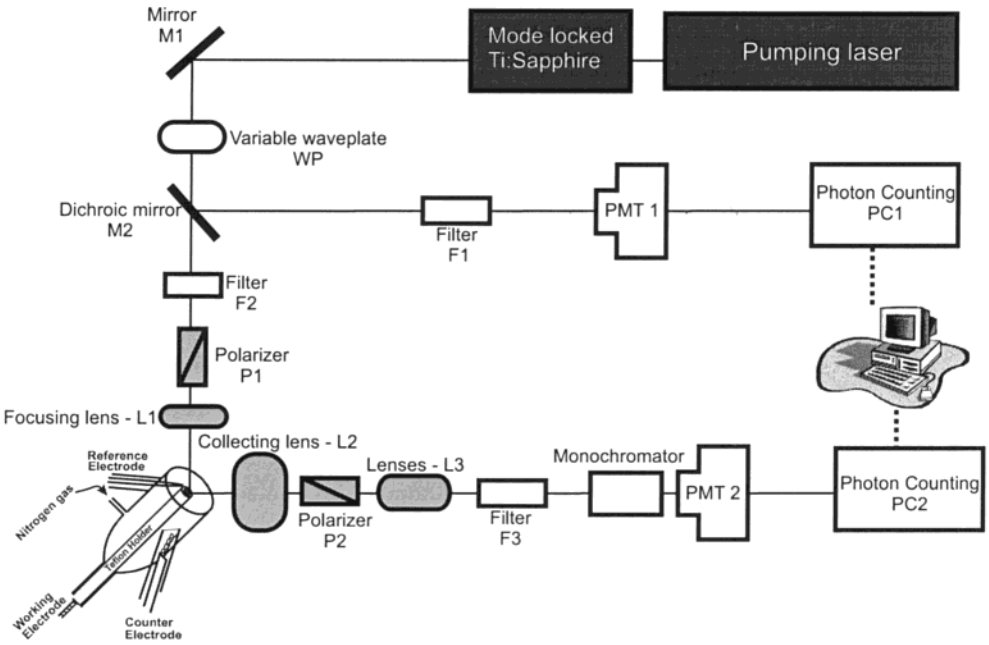

Figure 1. Experimental apparatus for electrochemical surface-enhanced second-harmonic generation measurements.

techniques allowed the unambiguous characterization of the potential-induced reorientation of the amino acid.

2. Experimental Section

2.1. Reagents and Solutions. The following reagents were used without further purification: KCl 99% (ACP) and L-cysteine 97% (Aldrich). The solutions were prepared using ultrapure water (18.2 MΩ) from a Barnstead NANOpure Diamond water purification system.

2.2. Cell, Electrodes, and Electrochemical Equipment. The working electrode was fabricated using a 99.99% silver rod (Premion, Alfa Aesar). A silver disk of ca. 6.35-mm diameter was mounted in a Teflon holder. Electrical contact was made to the silver electrode by an externally threaded stainless steel rod. Before each experiment, the working electrode was polished with emery paper and then with progressively finer grades of alumina powder down to 0.5 μm. The silver electrode was rinsed with copious amounts of ultrapure water and then transferred to the appropriate cell. A Ag/AgCl electrode was used as the reference, and all potentials in this paper are quoted against this reference. A 0.3-mm platinum wire (Alfa Aesar) was employed as the counter electrode. Electrochemical measurements were obtained using a computer-controlled Autolab potentiostat−galvanostat (PGSTAT30). The spectroelectrochemical cell used for both SERS and SESHG measurements has been described previously.[13] A Hokuto Denko potentiostat−galvanostat (HAB-151) and a Tektronix two-channel digital phosphor oscilloscope (TDS 3032) were used in all spectroelectrochemical experiments. The assembled cells were purged with prepurified N_2 for 30 min prior to the measurements, and a gentle stream of nitrogen was maintained to blanket the solution during data acquisition.

2.3. Activation Procedure. A rough silver surface is required for the observation of SERS and SESHG. The electrochemical protocol used to generate the necessary roughness is referred to as the activation procedure. In this work, the same method for surface preparation was used for both SERS and SESHG. Enhancement factors of at least 10^4 and 10^6 have been estimated for both SESHG and SERS, respectively.[13,14]

The activation procedure consisted of one oxidation−reduction cycle (ORC) performed on the polished silver electrode immersed in an aqueous solution containing 0.2 M KCl. The potential limits were −700 mV to +250 mV, and the scan rate was 5 mVs^{-1}. The applied potential was held during the reverse portion of the cycle immediately after the reduction of the silver ions (ca. −300 mV), and L-Cys was added to the system. Hence, the silver electrode was not oxidized in the presence of L-Cys. This procedure ensured that the organic molecule was neither trapped nor electrochemically degraded by the activation ORC.

2.4. Raman Instrumentation. Raman spectra were measured using a Dilor OMARS89 spectrometer coupled with an optical multichannel analyzer (OMA). The detector was a thermoelectrically cooled (ca. −15 °C) intensified diode array (512 diodes). The spectrometer was interfaced to an IBM PC-AT computer. The spectra were transferred to a Pentium computer containing the spectral manipulation routines. All SERS spectra were baseline-corrected and smoothed to average out the noise and improve the quality of the presentation. A Spectra Physics model 2020 argon ion laser was used as the excitation source. The spectra were obtained using the 514.5-nm line and 100 mW at the laser head. The acquisition time was 2 s, and a minimum of 100 accumulations were required for each spectrum. The laser light was chopped at 0.5 Hz, and background spectra were obtained and subtracted after each accumulation.

2.5. Surface Second-Harmonic Generation Instrumentation. Optical second-harmonic generation from the silver surface was obtained in situ in external reflection geometry. A schematic representation of the apparatus is presented in Figure 1. The pumping laser (Coherent Innova 400 Ar^+ ion laser) provided 15 W that was directed into the Ti/sapphire oscillator (Coherent Mira 900 F). The mode-locked Ti/sapphire oscillator produced a 76-MHz pulse train, but the repetition rate was trimmed by a pulse picker system to ca. 5 MHz. The working wavelength was 800 nm, the nominal pulse duration was 200 fs, and the pulse energy was on the order of 10 nJ. The laser light was redirected from the laser mirror M1 (CVI laser) into a variable waveplate (WP) (Karl Lambrecht). The crystal quartz of the Babinet Soleil compensator (WP) produced a small amount of second-harmonic radiation at 400 nm. This blue light was

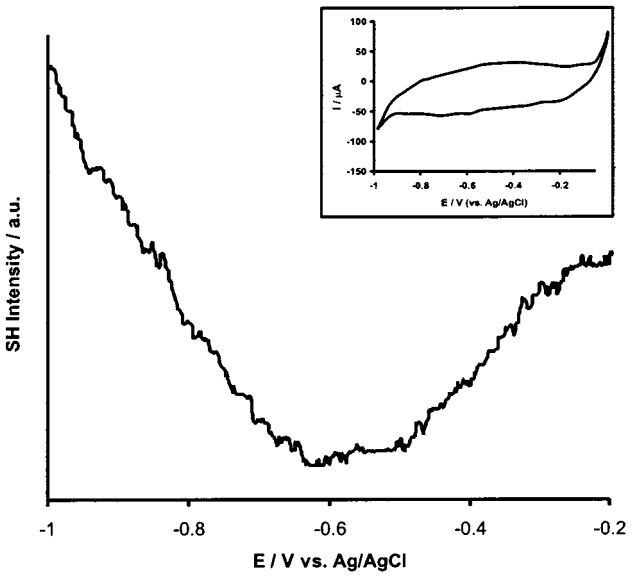

Figure 2. SESHG intensity vs applied potential plot (Ag/KCl = 0.2 M, no L-Cys present, obtained at 5 mV s^{-1}). The inset shows a cyclic voltammogram for this system.

reflected from the harmonic separator M2 (CVI) into a spectroscopic cell containing a $CuSO_4$ solution (filter F1 in Figure 1). This cell filtered out the residual near-infrared light (800 nm) and allowed only the second-harmonic component (400 nm) to reach the photomultiplier detector (PMT 1). The 400-nm light detected at PMT 1 was used as a reference to correct for any eventual fluctuations of the laser power throughout the experiments. The light transmitted from the dichroic separator M2 propagated into a narrow-band interference filter F2 (CVI). F2 allowed only 800-nm light to reach the polarizer P1 (Glan Laser, CVI). Light with the polarization vector parallel to the physical plane of incidence (p-polarized, as defined in ref 15) was used in all experiments. The near-infrared light was focused from a lens L1 (5-cm focal length) to the metallic surface. We estimated that the laser power density on the surface was on the order of 5 MW cm^{-2}. This power density is below the typical damage threshold for metallic surfaces, and indications of surface degradation provoked by the laser were not observed either in the presence or in the absence of adsorbed L-Cys. The reflected light from the surface was collected by a 50-mm photographic lens L2 (Canon) and directed into the polarizer P2 (Glan Laser, CVI) for the selection of the p-polarized component. The diffuse light reflected from the rough silver surface was found to be completely isotropic in terms of polarization, and the polarizer P2 was further removed from the setup. A 5-mm diameter beam was collimated into the $CuSO_4$ filter F3 by the lens system L3 (the lenses L2 and L3 are not necessary when the experiment is performed using a smooth metallic surface). Any residual near-infrared light after F3 was further separated by a 20-cm monochromator (Bausch & Lomb). The second-harmonic component generated from the surface was detected by PMT 2. Both PMT 1 and PMT 2 were housed in a thermoelectric refrigerated chamber (Products for Research) and operated at ca. −20 °C. The photon counting systems (PC1 and PC2) consisted of an amplifier/discriminator (PAR) and a high-speed ratemeter (PAR). The PAR ratemeters also provided the required high voltage for the operation of the PMTs. The analog readings from the photon-counting systems were fed to a Pentium computer equipped with a data acquisition board (PCI 6024E, National Instruments (NI)) and a connector accessory (BNC 212, NI). The signal from the silver surface and the reference SH from the crystal quartz of the compensator were digitized using customized data acquisition software written in LabView (NI). This software also recorded the electrochemical information from the oscilloscope and the second-harmonic signals simultaneously.

3. Results and Discussion

3.1. Surface-Enhanced Second-Harmonic Generation from the Ag/KCl 0.2 M Interface. The dependence of the SESHG signal on the applied potential for a rough silver electrode in 0.2 M KCl (in the absence of L-Cys) is presented in Figure 2. The inset in Figure 2 shows a cyclic voltammogram (CV) for the rough silver electrode. The CV for the rough electrode displayed a larger capacitive current in the double-layer region compared to that of the smooth (freshly polished) silver surface (not shown). The hydrogen evolution reaction was found to start at potentials more negative than −900 mV.

The potential dependence of the second-harmonic signal generated from an electrified interface is expected to be parabolic, with a minimum around the potential of zero charge (pzc).[16] Parabolic behavior is clearly followed around the minimum of the curve presented in Figure 2. However, the pzc from a rough silver electrode in the presence of KCl was determined to be around −900 mV.[17,18] In fact, the positions of the pzc for both the rough and smooth silver surfaces in the presence of chloride have been established to be essentially the same by differential capacitance measurements.[17,19] Hence, the potential where the minimum in the SESHG signal occurs in Figure 2 is approximately 300 mV more positive than expected for the pzc of a polycrystalline silver electrode. Figure 2 is, however, in very good agreement with the results reported by Richmond and collaborators[20,21] for silver electrodes under similar experimental conditions. A comparable curve was also obtained in a surface plasmon-enhanced SHG experiment from a polycrystalline silver film−aqueous solution interface using attenuated total reflection (ATR) geometry.[22] The potential dependence of the second-harmonic intensity generated from rough silver surfaces (Figure 2 and refs 20 and 21) is in remarkable contrast with the observations from smooth silver surfaces in the same medium.[20,23] In general, the second-harmonic signal from a smooth silver surface follows the parabolic law, with a minimum that is close to the pzc.

The experiments from ref 20 were performed using excitation at 1064 nm, and Figure 2 was obtained using excitation at 800 nm. Both experimental conditions yielded essentially the same potential dependence for the SESHG signal, which is an indication that the curve presented in Figure 2 is not a consequence of electronic resonance effects that are commonly operative in SERS (CT mechanism).[13]

The rough silver surface structures allow for the excitation of localized surface plasmon that significantly enhances the local electromagnetic field.[24] The magnitude of this electromagnetic enhancement is dependent on the dielectric properties of the interface and, consequently, on the energy of the incident radiation. We are not aware of any theoretical framework that can fully explain the potential dependence of the SESHG from silver interfaces in halide media as presented in Figure 2 and refs 20 and 21. However, because the behavior presented in Figure 2 is a consequence of a plasmon-mediated mechanism for second-harmonic generation, the effect should be very sensitive to the electronic characteristics of the electrode surface. Hence, changes in the chemical nature of the adsorbate are expected to modify the potential dependence of the SESHG intensities significantly.

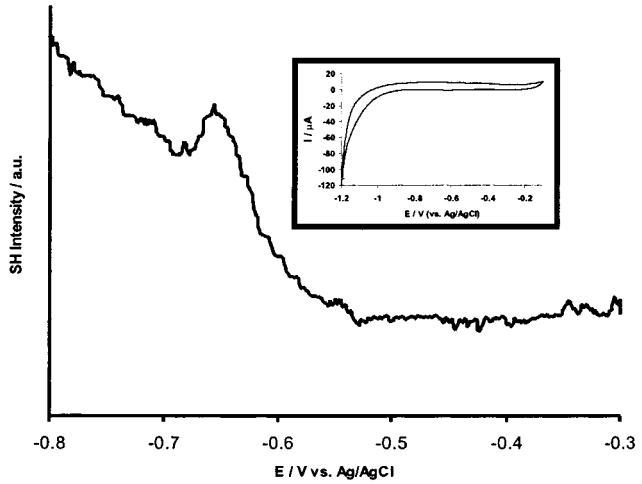

Figure 3. SESHG intensity vs applied potential plot (Ag/KCl = 0.2 M, [L-Cys] = 5×10^{-2} M, obtained at 5 mV s^{-1}). A cyclic voltammogram for this system is shown in the inset.

3.2. Surface-Enhanced Second-Harmonic Generation and Surface-Enhanced Raman Scattering from the Ag/KCl 0.2 M Interface in the Presence of L-Cys. L-Cys was added to the spectroelectrochemical cell to give a final concentration of 5×10^{-2} M. The addition was made at constant potential (−300 mV) after the first ORC. No ORC was performed in the presence of L-Cys. The cyclic voltammogram obtained after L-Cys addition (inset of Figure 3) shows a decrease in the capacitive current in the double-layer region compared to the CV obtained in the absence of L-Cys (inset in Figure 2). The attenuation of the double-layer capacity occurs because a compact (blocking) layer is formed as L-Cys adsorbs at that potential. No faradaic peak or any electrochemical indication of desorption is present in the CV between −300 and −800 mV, suggesting that L-Cys remains adsorbed on the silver surface within this potential range. The onset of the hydrogen evolution reaction occurs after −900 mV.

Figure 3 displays the dependence of the SESHG signal on the applied potential in the presence of L-Cys. The SESHG was measured between −300 and −800 mV to avoid any faradaic process. It is clear that the presence of L-Cys considerably modifies the optical nonlinear response of the interface.

The second-harmonic signal from Figure 3 does not change significantly between −300 mV and ca. −550 mV, which can be explained by considering that the free-electron contribution is predominant in that range. The adsorption of L-Cys on a silver electrode occurs through dissociative oxidation leading to the formation of a strong silver−sulfur bond. The formation of the Ag−S bond localizes the electron from the metal, thus minimizing the free-electron contribution to the second harmonic in that potential range. This result is in accordance with the decrease of the second-harmonic signal generated from a polycrystalline gold electrode because of the adsorption of *n*-alkyl thiols.[25] An increase in the SESHG from Figure 3 is observed as the potential becomes more negative than ca. −550 mV. This behavior is similar to that observed after the minimum in Figure 2 and must be associated with the same plasmon-mediated mechanism. A well-defined peak is apparent when the potential reaches ca. −650 mV. This peak should be related to an abrupt disturbance in the electronic characteristics of the interface, suggesting either a structural rearrangement or a sudden compositional change of the monolayer. The SESHG signal gradually increases linearly after the peak until −800 mV (Figure 3). The reverse scan (not shown) presented some hysteresis, but the same features described above were also always observed.

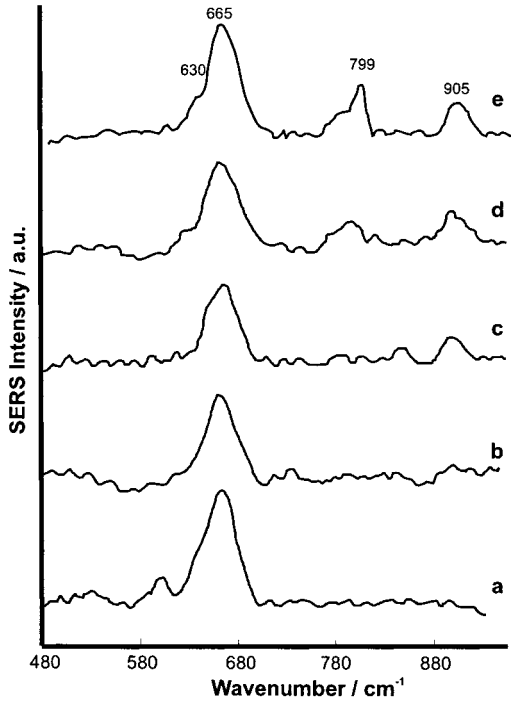

Figure 4. SERS spectra at different applied potentials (Ag/KCl = 0.2 M, [L-Cys] = 5×10^{-2} M). (a) *E* (mV) = −300, (b) −450, (c) −600, (d) −700, (e) −850.

The SERS spectra for L-Cys adsorbed on the electrochemically roughened silver electrode at different applied potentials are presented in Figure 4. The band at ca. 665 cm^{-1} was predominant for potentials more positive than −600 mV (Figure 4a−c). This band can be assigned to the C−S stretching mode. The frequency of this mode is red-shifted from around 690 cm^{-1} for L-Cys in solution.[10,11] This shift indicates that the sulfur atom of L-Cys should be directly bonded to the surface. New SERS bands are apparent in Figure 4 as the potential becomes more negative than −600 mV (Figure 4d,e). The appearance of these new SERS bands coincides with the peak in Figure 3 (around −650 mV). The SERS intensity for the C−S stretching mode does not change significantly as the potential becomes negative, indicating that L-Cys does not leave the Ag surface in the potential range studied. This conclusion is supported by the lack of a defined desorption peak on the cyclic voltammogram obtained in the presence of L-Cys (inset in Figure 3). There are two possibilities for the new SERS bands observed at potentials more negative than −600 mV (as for the peak in Figure 3). These bands may either be due to the reorientation of L-Cys molecules or to the cathodic decomposition of the amino acid. The absence of cathodic peaks in the cyclic voltammogram obtained in the presence of L-Cys goes against the hypothesis of electrochemical decomposition. Moreover, all spectral features observed at potentials more negative than −600 mV (Figure 4d and e) can be assigned to L-Cys vibrations.[10−12,26] The shoulder at 630 cm^{-1} and the peaks at 799 and 905 cm^{-1} can be related to the COO^- wagging, the COO^- bending, and the C−COO^- stretching, respectively. All of the new SERS bands involved vibrational modes related to the carboxylate group.

Considering the sulfur atom attached to the surface, we found that three conformations are possible for the relative orientations of the amino and the carboxylate groups. The Newman projections of these rotamers are presented in Figure 5. The possibility of eclipsed conformations was not considered because the energy of these rotamers should be prohibitively high. L-Cys

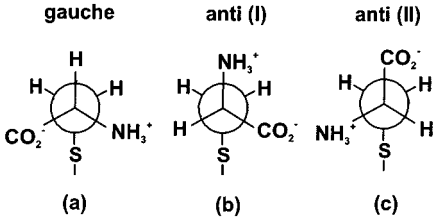

Figure 5. Newman projections for the possible conformations of adsorbed L-Cys.

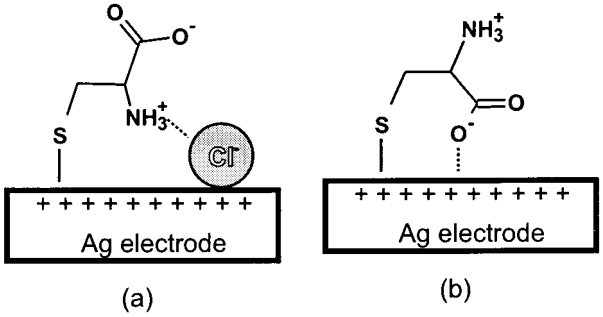

Figure 6. Model for the adsorption of L-Cys on a polycrystalline silver electrode. (a) Adsorption geometry at potentials more positive than −650 mV (in the presence of coadsorbed Cl^- ions). (b) Adsorption geometry at potentials more negative than −650 mV (in the absence of coadsorbed Cl^-).

exists in its zwitterionic form under the conditions of these experiments (pH ≅ 6). The gauche conformation (Figure 5a) is found in orthorhombic L-Cys crystals.[27] The anti (I) conformation (Figure 5b) and the gauche conformation (Figure 5a) are found in monoclinic L-Cys crystals.[28] The relative populations of the staggered rotameric forms of L-Cys in aqueous solution at different pH conditions have been observed by NMR.[29,30] The gauche conformation (Figure 5a) was found to be predominant in acidic media. This rotamer is also present in appreciable amounts in basic media, but the anti (II) configuration (Figure 5c) is the dominant species.

A vibrational normal-mode analysis of L-Cys has been carried out.[31] According to the calculations, Raman frequencies can be used to identify specific rotamers of L-Cys in solution.[31] Unfortunately, the conformation-sensitive modes are the C−S stretch and the S−H stretch. Neither of these modes can be used for the identification of the conformation of adsorbed L-Cys. The oxidative adsorption of L-Cys on silver breaks the S−H bond, and the C−S mode is already strongly perturbed by the presence of the surface.

The increase in the SERS intensity of carboxylate modes (such as the ones observed in Figure 4) at higher pH was taken as an indication of a strong interaction between the COO^- group and the surface.[10] Using similar arguments, it is possible to understand both the SERS and SESHG features in terms of conformational changes driven by the applied potential. The absence of SERS bands due to the carboxylate group indicated that the anti (II) conformation (Figure 5c) is dominant at potentials more positive than ca. −650 mV. This conclusion may seem contradictory because the electrode surface is positively charged at these potentials and the carboxylate group is negatively charged. Nevertheless, the L-Cys molecule is certainly coadsorbed with chloride anions.[18] This situation is illustrated in Figure 6a. The simultaneous adsorption of the anion and the organic analyte is observed in all SERS experiments performed in the presence of halides.[32] The chloride ions should attract the protonated amino group (positively charged) to the surface and drive the carboxylate group away, favoring the anti (II) conformation depicted in Figure 6a. The chloride ions are expelled from the surface as the potential becomes negative. The still positively charged surface (the pzc is around −900 mV[18]) should be attractive to the carboxylate group, as represented in Figure 6b. The replacement of chloride by carboxylate groups can be thought of in terms of simple electrostatic arguments. The positive value of the surface charge decreases as the potential is swept to negative values. The delocalized negative charge in the carboxylate should interact better with this less positively charged surface (Figure 6b) than with chloride ions. The SERS bands observed in Figure 4 for potentials more negative than −600 mV is a clear consequence of the close proximity between the carboxylate group and the surface. The configurational change of the adsorbed L-Cys on silver surfaces is corroborated by the SESHG results presented in Figure 3. The SESHG signal increases from ca. −550 mV as the chloride leaves the surface. The proposed reorientation would bring another negatively charged species (carboxylate) into direct contact with the surface, provoking a sudden change in the electronic characteristics of the interface. The adsorbed L-Cys conformers presented in Figure 5a and b have the COO^- close to the surface and could be responsible for the spectral changes at potentials more negative than ca. −650 mV.

4. Conclusions

This work demonstrated that L-Cys strongly adsorbs on a silver electrode and that the amino acid molecules do not leave the surface even at potentials as negative as −900 mV. The SERS and SESHG results indicated that the L-Cys molecules have distinct orientations at different applied potentials. The carboxylate group is kept away from the surface at potentials more positive than ca. −650 mV, which is a consequence of the coadsorption of chloride ions that interact favorably with the protonated amino group and repel the carboxylate. The chloride ions leave the surface as the potential is swept to negative values, allowing a conformational change that brings the carboxylate group closer to the surface. This reorientation provokes a dramatic change in the SESHG intensity versus applied potential curve. The significant response of the SESHG signal due to the reorientation demonstrates that this technique is indeed very sensitive to small changes in the electronic characteristics of the interface. However, a simple relationship between the SESHG and the applied potential could not be inferred from the experimental curves (even in the absence of L-Cys). It is clear that this method would certainly benefit from some theoretical development on the treatment of the potential dependence of surface plasmon-enhanced phenomena. The proposed reorientation was confirmed by SERS. The SERS bands of the carboxylate group are clearly present at potentials more negative than −650 mV. A direct relationship between the potential-dependent SESHG signal and the number of adsorbed molecules was not observed.

Acknowledgment. This research was supported by grants from the University of Victoria (Start Up grant), the Canada Foundation for Innovation (CFI), and the British Columbia Knowledge Development Fund (BCKDF). A.G.B. thanks Dr. Donald E. Irish for the donation of the Raman equipment. We also thank L. Netter for help with the development of the LabView program used for the data acquisition.

References and Notes

(1) Ralph, T. R.; Hitchman, M. L.; Millington, J. P.; Walsh, F. C. *J. Electroanal. Chem.* **1994**, *375*, 1.

(2) Tengvall, P.; Liedberg, B.; Ludstrom, I. *Langmuir* **1992**, *8*, 1236.
(3) (a) Heyrovsky, M.; Vavricka, S. *Biochem. Bioenerg.* **1999**, *48*, 43. (b) Spataru, N.; Sarada, B. V.; Popa, E.; Tryk, D. A.; Fujishima, A. *Anal. Chem.* **2001**, *73*, 514. (c) Tudos, A. J.; Vandeberg, P. J.; Johnson, D. C. *Anal. Chem.* **1995**, *67*, 552. (d) Tudos, A. J.; Johnson, D. C. *Anal. Chem.* **1995**, *67*, 557. (e) Xie, Q.; Zhang, Y.; Yuan, Y.; Guo, Y.; Wang, X.; Yao, S. *J. Electroanal. Chem.* **2000**, *484*, 41. (f) Arrigan, D. W. M.; Le Bihan, L. *Analyst* **1999**, *124*, 1645.
(4) (a) Fawcett, W. R.; Ferduco, M.; Kovacova, Z.; Borkowska, Z. *J. Electroanal. Chem.* **1994**, *368*, 265. (b) Fawcett, W. R.; Ferduco, M.; Kovacova, Z.; Borkowska, Z. *J. Electroanal. Chem.* **1994**, *368*, 275. (c) Fawcett, W. R.; Ferduco, M.; Kovacova, Z.; Borkowska, Z. *Langmuir* **1994**, *10*, 912.
(5) Dakkouri, A. S.; Kolb, D. M.; Edelstein-Shima, R.; Mantler, D. *Langmuir* **1996**, 12, 2849.
(6) Zhang, J.; Chi, Q.; Nilsen, U.; Friis, E. P.; Andersen, J. E. T.; Ulstrup, J. *Langmuir* **2000**, *16*, 7229.
(7) Xu, Q.-M.; Wan, L.-J.; Wang, C.; Bai, C.-L.; Wang, Z.-Y.; Nozawa, T. *Langmuir* **2001**, *17*, 6203.
(8) Ihs, A.; Liedberg, B. *J. Colloid Interface Sci*. **1991**, *144*, 282.
(9) Uvdal, K.; Bodo, P.; Liedberg, B. *J. Colloid Interface Sci.* **1992**, *149*, 162.
(10) Lee, H.; Kim, M. S.; Suh, S. W. *J. Raman Spectrosc.* **1991**, *22*, 91.
(11) Watanabe, T.; Maeda, H. *J. Phys. Chem.* **1989**, *93*, 3258.
(12) Stewart, S.; Fredericks, P. M. *Spectrochim. Acta, Part A* **1999**, *55*, 1641.
(13) Brolo, A. G.; Irish, D. E.; Smith, B. D. *J. Mol. Struct.* **1997**, *405*, 29.
(14) Chen, C. K.; Castro, A. R. B.; Shen, Y. R. *Phys. Rev. Lett.* **1981**, *46*, 145.
(15) Bard, A. J.; Faulkner, L. R. *Electrochemical Methods: Fundamentals and Applications*, 2nd edition; Wiley: New York, 2001; Chapter 17, p 687.
(16) Pettinger, B.; Bilger, C.; Lipkowski, J.; Schmickler, W. In *Interfacial Electrochemistry: Theory, Experiment, and Applications*; Wieckowski, A., Ed.; Marcel Dekker: New York, 1999; Chapter 22, p 373.
(17) Larkin, D.; Guyer, K. L.; Hupp, J. T.; Weaver, M. J. *J. Electroanal. Chem.* **1982**, *138*, 401.
(18) Hupp, J. T.; Larkin, D.; Weaver, M. J. *Surf. Sci.* **1983**, *125*, 429.
(19) Weaver, M. J.; Barz, F.; Gordon, J. G., II; Philpott, M. R. *Surf. Sci.* **1983**, *125*, 409.
(20) Rojhantalab, H. M.; Richmond, G. L. *J. Phys. Chem.* **1989**, *93*, 3269.
(21) Richmond, G. L. *Langmuir* **1986**, *2*, 132.
(22) Corn, R. M.; Romagnoli, M.; Levenson, M. D.; Philpott, M. R. *Chem. Phys. Lett.* **1984**, *106*, 30.
(23) Aktsipetrov, O. A.; Melnikov, A. V.; Murzina, T. V.; Nikulin, A. A.; Rubtsov, A. N. *Surf. Sci.* **1995**, *336*, 225.
(24) Chen, C. K.; Heinz, T. F.; Ricard, D.; Shen, Y. R. *Phys. Rev. B: Condens. Matter* **1983**, *27*, 1965.
(25) Buck, M.; Grunze, M.; Eisert, F.; Fischer, J.; Trager, F. *J. Vac. Sci. Technol., A* **1992**, *10*, 926.
(26) Gargaro, A. R.; Barron, L. D.; Hecht, L. *J. Raman Spectrosc.* **1993**, *24*, 91.
(27) Kerr, K. A.; Ashmore, J. P. *Acta Crystallogr., Sect. B* **1973**, *29*, 2124.
(28) Harding, M. M.; Long, H. A. *Acta Crystallogr., Sect. B* **1968**, *24*, 1096.
(29) Bartle, K. D.; Jones, D. W.; L'Amie, R. *J. Chem. Soc., Perkin Trans. 2* **1972**, 646.
(30) Dale, B. J.; Jones, D. W. *Spectrochim. Acta, Part A* **1975**, *31*, 83.
(31) Li, H.; Wurrey, C. J.; Thomas, G. J., Jr. *J. Am. Chem. Soc.* **1992**, *114*, 7463.
(32) Brolo, A. G.; Irish, D. E. *J. Electroanal. Chem.* **1996**, *414*, 183.